Arsenic quantification in seafood material within the CCQM APMP.QM-S19 comparison

M. Di Luzio, L. Bergamaschi, M. Santiano, M. Oddone, G. D'Agostino

Arsenic quantification in seafood material within the CCQM APMP.QM-S19 comparison

T.R. 21/2022 May 2022

RAPPORTO TECNICO I.N.RI.M.

1. Abstract

The aim of this analysis is the quantification of As mass fraction in an organic matrix, performed by Instrumental Neutron Activation Analysis (INAA) carried out with relative standardization. The sample to investigate consists of dried shrimp material and is provided by the Government Laboratory, Hong Kong, (GLHK) in the framework of the CCQM APMP.QM-S19 supplementary comparison. This document describes the detailed procedure adopted in the analysis together with the obtained results and a final discussion concerning the total uncertainty budget (i. e. the budget including information from all the replicates measured in the analysis).

2. Experimental

The experimental procedure adopted in the analysis consisted in the application of a relative-standardization INAA performed on 9 aliquots of the material taken from a 30 g bottle. All available information was used to evaluate the As mass fraction in the investigated material.

2.1 Samples preparation

The 30 g mass powder contained in the bottle provided for the comparison (Figure 1, left) was carefully mixed by flipping over several times and aliquots of dried shrimp material were taken and pressed to get cylindrical tablets with 10 mm diameter (Figure 1, right) after application of a 15 bar pressure by a manual hydraulic press (Figure 1, center).

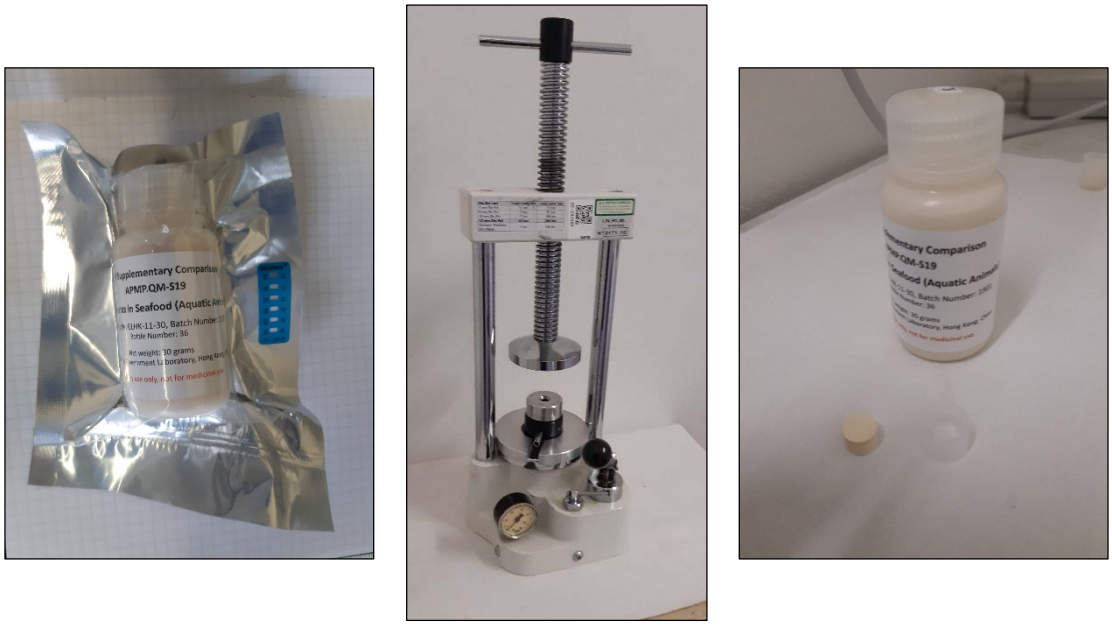

Figure 1: The comparison material (left), the manual hydraulic press used to prepare samples (center) and a pressed cylindrical tablet sample (right).

After brief inspection for visible cracks, each tablet was placed in a cleaned 3 mL PE irradiation vial, cut to about 10 mm height, and weighted on a calibrated analytical balance Mettler AX105 (Figure 2, left). Before taking measurements, the balance was checked using a SI traceable weight set Cibe (Figure 2, right).

Figure 2: The calibrated analytical balance used to measure the mass (left) and the SI traceable weight set (right).

A further aliquot was pressed into a tablet with the same procedure adopted to obtain the 9 samples. Its 6.5(1) mm height, h_{smp}, was measured with a caliper and adopted for all samples; here and hereafter, value in parenthesis indicate the standard uncertainty referred to the corresponding last digit unless differently specified.

Moisture mass fraction, η_{smp}, was evaluated using two different procedures at the same time than sample preparation: (i) by drying with anhydrous calcium sulphate (Figure 3, left) and (ii) by heating with a Mettler thermo-balance (Figure 3, right).

Figure 3: The desiccators (left) and the thermo-balance (right) used to measure the moisture mass fraction.

In the first case, (i), three 1 g aliquots of the material were weighted with the analytical balance and kept in a desiccator for more than 10 days and then weighted; the procedure was repeated until negligible mass variations were observed between subsequent measurements. Since the desiccated material was highly hygroscopic, a correction was applied to deal with the moisture gained back while the sample was lying on the balance plate during mass measurement. The correction was calculated by applying a parabolic fit to the

sample mass increase versus time registered after short and regular intervals. In the second case, (ii), three 1 g aliquots of the material were weighted on the thermo-balance and heated up to 105 °C until negligible mass variation (0.02 % in 120 s) was reached.

The η_{sm} value was calculated as the average of three measurements reported in Table 1 and resulted to be 5.3(2) % or 5.9(2) % in case of use of the procedure (i) or (ii), respectively. As prescribed in the instructions of the comparison, the value obtained by the procedure (i) was adopted for further calculations.

Table 1: Moisture mass fraction values measured using both (i) the desiccator and (ii) themo-balance methods. The value in parenthesis indicate the standard uncertainty referred to the corresponding last digit.

Sample n.	η_{sm} (i) / %	η_{sm} (ii) / %
1	5.26	5.73
2	5.33	5.93
3	5.16	5.92
Average	5.3(2)	5.9(2)

2.2 Standards preparation

A SI traceable As solution was used to prepare 12 As standards for the relative-INAA setup. The solution was pipetted on 6 mm diameter absorbent paper disc previously attached to a 10 mm diameter polyethylene (PE) adhesive tape disk. The pipetting process was performed on the analytical balance in order to keep track of the pipetted mass. Since evaporation from the pipetted solution was noticeable, a correction was performed to calculate the mass value at the time the solution was dropped on filter paper: a linear correction was applied based on the evaporation rate evaluated by measuring the mass decrease registered after short and regular intervals. After weighing, the solution was completely evaporated under a fume hood and a second 10 mm diameter polyethylene (PE) adhesive tape disk was used to seal the standard. The 0.10(5) mm height of a standard, h_{std}, was measured with a caliper and adopted for all standards;

A standard, consisting of a disc of absorbent paper with a known mass of As sealed between two foils of adhesive tape, is shown in Figure 4.

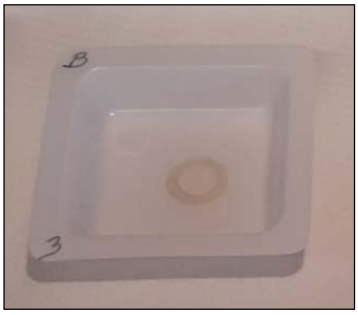

Figure 4: An As standard disk.

2.3 Neutron irradiation

The 9 samples and the 12 As standards are shown in Figure 5.

Figure 5: The 9 cylindrical tablet samples in their cut 3 mL PE irradiation vials and the 12 As standard discs.

Samples and As standards were distributed in three 8 mL PE irradiation containers, called A, B and C, suitably cut to keep the positioning fixed. In details, 3 samples and 4 As standards were placed in each irradiation container together with a dummy cut 3 mL PE vial as represented in Figure 6; codes representing the unique identification tag assigned to each item and the corresponding names indicating the content of each item are reported in Table 2 together with the distance, *d*, between standards.

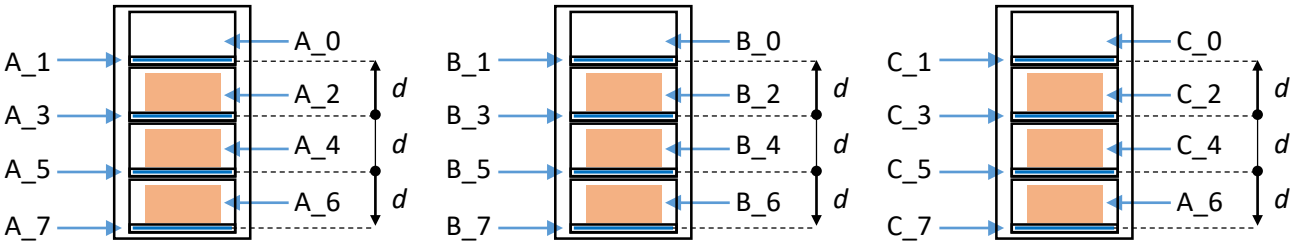

Figure 6: Position of samples and standards within their irradiation containers A, B and C, respectively. Code and corresponding name and *d* values are reported in Table 2.

As standard disks were inserted within the internal hollow at the bottom of each sample irradiation vial in order to leave the minimum possible distance (about 1 mm) between the bottom of sample and its standard. The height of each sample irradiation vial was measured with a caliper and adopted as the distance *d* between As standard samples. The picture of an irradiation container filled in with samples and standards is shown in Figure 7. The 3 samples are noticeable (darker shadow) whereas the 4 standards are unnoticeable.

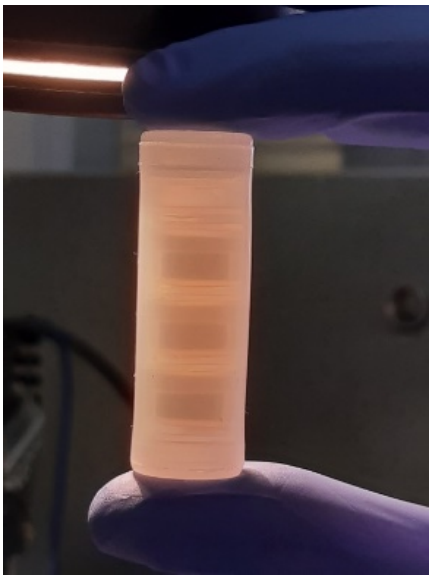

Figure 7: Picture of a cut 8 mL irradiation container filled in with samples.

Sample height, *h*, mass, *m*, moisture mass fraction, *η*, and densities, *ρ*, calculated from mass and volume are reported in Table 2.

Table 2: Code and sample names of the three cut 8 mL PE irradiation vials, A, B and C, prepared for neutron exposure. Sample height, *h*, mass, *m*, moisture mass fraction, *η*, distance between standards, *d*, and densities, *ρ*, are also reported. The value in parenthesis indicate the standard uncertainty referred to the corresponding last digit.

code	sample	*h* / mm	*m* / g	*η* / 1	*d* / mm	*ρ* / g cm^{-3}
A_0	*dummy*	-				
A_1	*As standard*	0.10(5)	0.03083(2)	-		0.010(2)
A_2	*shrimp sample*	6.5(1)	0.53206(1)	5.3(2) %	10.7(2)	1.00(2)
A_3	*As standard*	0.10(5)	0.03119(2)	-		0.010(2)
A_4	*shrimp sample*	6.5(1)	0.54270(1)	5.3(2) %	10.6(2)	1.10(2)
A_5	*As standard*	0.10(5)	0.03113(2)	-		0.010(2)
A_6	*shrimp sample*	6.5(1)	0.55115(1)	5.3(2) %	10.8(2)	1.10(2)
A_7	*As standard*	0.10(5)	0.03035(2)	-		0.010(2)

code	sample	*h* / mm	*m* / g	*η* / 1	*d* / mm	*ρ* / g cm^{-3}
B_0	*dummy*	-				
B_1	*As standard*	0.10(5)	0.03105(2)	-		0.010(2)
B_2	*shrimp sample*	6.5(1)	0.54247(1)	5.3(2) %	10.6(2)	1.10(2)
B_3	*As standard*	0.10(5)	0.03055(2)	-		0.010(2)
B_4	*shrimp sample*	6.5(1)	0.55141(1)	5.3(2) %	10.7(2)	1.10(2)
B_5	*As standard*	0.10(5)	0.03115(2)	-		0.010(2)
B_6	*shrimp sample*	6.5(1)	0.55687(1)	5.3(2) %	10.9(2)	1.10(2)
B_7	*As standard*	0.10(5)	0.03109(2)	-		0.010(2)

code	sample	*h* / mm	*m* / g	*η* / 1	*d* / mm	*ρ* / g cm^{-3}

C_0	*dummy*	-				
C_1	*As standard*	0.10(5)	0.03104(2)	-		0.010(2)
C_2	*shrimp sample*	6.5(1)	0.55086(1)	5.3(2) %	10.9(2)	1.10(2)
C_3	*As standard*	0.10(5)	0.03025(2)	-		0.010(2)
C_4	*shrimp sample*	6.5(1)	0.55083(1)	5.3(2) %	10.5(2)	1.10(2)
C_5	*As standard*	0.10(5)	0.03072(2)	-		0.010(2)
C_6	*shrimp sample*	6.5(1)	0.51963(1)	5.3(2) %	10.4(2)	1.00(2)
C_7	*As standard*	0.10(5)	0.03121(2)	-		0.010(2)

The irradiation took place in the TRIGA Mark II reactor of the University of Pavia; containers A, B and C were placed in three cartridge cases and sent to channels 25, 26 and 27 of the Lazy Susan facility, respectively; the neutron exposure lasted 6 non-continuous hours at maximum 250 kW power.

2.4 Gamma spectrometry

Irradiated cartridge cases were collected on the second day after the end of irradiation. Samples and standards were carefully extracted from their cut 8 mL irradiation containers. The cut 3 mL samples were placed in gamma counting containers and centered with hollow discs suitably shaped to assure axial positioning within tenths of mm. Each standard was first inserted in cut 3 mL PE vial to position the disk at a distance equivalent to the bottom of a sample and then placed and centered in gamma counting containers with additional hollow disks. The position of sample and standard within their gamma counting containers is shown in Figure 8.

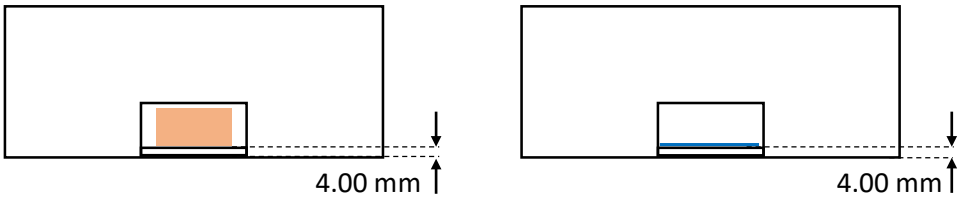

Figure 8: Position of sample (left) and standard (right) within their gamma counting container.

Gamma spectrometry was performed with a HyperPure germanium (HPGe) detector ORTEC GEM50P4-83 (50 % relative efficiency, 1.9 keV full-width half maximum at 1332.5 keV energy) connected to multichannel analyzer ORTEC DSPEC 502 and controlled by a personal computer. The detection system was extensively characterized in terms of efficiency using a mix of single nuclide γ-sources with SI traceable activity measured at nominal counting positions d_{200}, d_{180}, d_{160}, d_{140}, d_{120}, d_{100}, d_{80}, d_{60}, d_{40} and d_{20} located at 203.6 mm, 183.6 mm, 163.6 mm, 143.6 mm, 123.6 mm, 103.6 mm, 83.6 mm, 63.6 mm, 43.6 mm and 23.6 mm from the detector endcap, respectively. Nominal counting positions were identified with vertical spacers having 200 mm, 180 mm, 160 mm, 140 mm, 120 mm, 100 mm, 80 mm, 60 mm, 40 mm and 20 mm heights that were specifically crafted to comfortably place the counting containers while assuring knowledge on vertical distance within tenths of mm. The characterized nominal counting positions are shown in Figure 9.

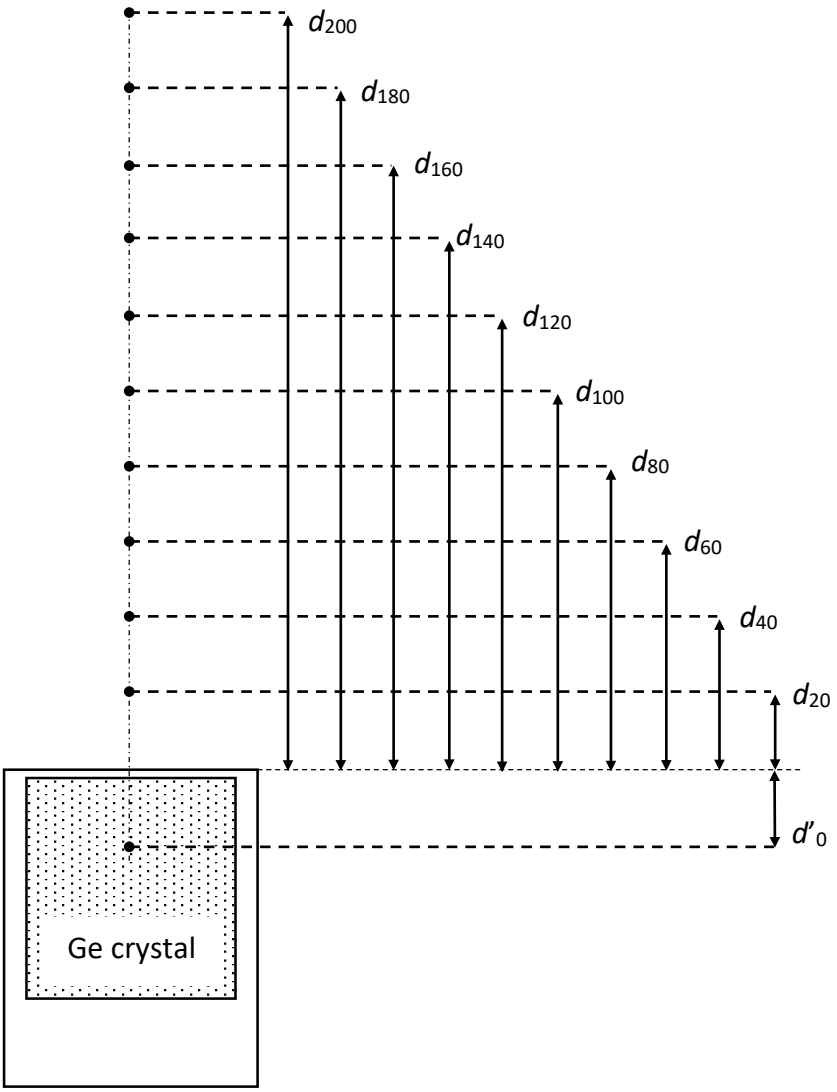

Figure 9: Location of the nominal counting positions d_{200}, d_{180}, d_{160}, d_{140}, d_{120}, d_{100}, d_{80}, d_{60}, d_{40} and d_{20} located at 203.6 mm, 183.6 mm, 163.6 mm, 143.6 mm, 123.6 mm, 103.6 mm, 83.6 mm, 63.6 mm, 43.6 mm and 23.6 mm from the detector endcap, respectively. The distance of the point-of-action, d'_0, is also indicated.

For each of the 9 sample-standard pairs A_2-A_3, A_4-A_5, A_6-A_7, B_2-B_3, B_4-B_5, B_6-B_7, C_2-C_3, C_4-C_5 and C_6-C_7, two gamma spectrometry measurements were performed: the first one at d_{80} and the latter at d_{40}. The measurement was repeated to check the data quality; the closer counting position was necessary to counterbalance the As decay. The acquisitions were performed at fixed real counting time, ranging from 30 to 70 minutes, in order to conclude the gamma counting of the whole series of samples (or standards) acquisitions within a single work day.

The counting spacers used for the d_{80} and d_{40} nominal positions are shown in Figure 10.

Figure 10: Counting spacers for d_{80} (left) and d_{40} (right) nominal positions. The gamma counting container with the cut 3 mL PE vial centered by the hollow disk is visible on top of the d_{40} spacer.

3. Data elaboration

Collected gamma spectra were elaborated with HyperLab 2014 software to get ^{75}As 559.1 keV net peak areas. Gamma spectra, peak lists and additional input parameters were processed with the Rel-INRIM software, homemade developed, to produce uncertainty budgets of elemental mass fractions based on relative-INAA standardization.

The measurement model was obtained starting from the equation developed for the k_0-INAA standardization described in [1] suitably adjusted to quantify an element in a sample, smp, using a standard, std, of the same element. The resulting equation, including 38 input quantities, is:

$$w_{\mathrm{smp}} = \left(\frac{\frac{n_{\mathrm{p\,smp}}\, t_{\mathrm{c\,smp}}\, e^{\mu\left(1-t_{\mathrm{l\,smp}}/t_{\mathrm{c\,smp}}\right)}}{t_{\mathrm{l\,smp}}\left(1-e^{-\lambda t_{\mathrm{c\,smp}}}\right)}}{\frac{n_{\mathrm{p\,std}}\, t_{\mathrm{c\,std}}\, e^{\mu\left(1-t_{\mathrm{l\,std}}/t_{\mathrm{c\,std}}\right)}}{t_{\mathrm{l\,std}}\left(1-e^{-\lambda t_{\mathrm{c\,std}}}\right)}}\; e^{\lambda\,\Delta t_{\mathrm{d}}}\, \frac{1}{1+\beta\,\Delta l}\, \frac{G_{\mathrm{th\,std}}+\frac{G_{\mathrm{e\,std}}}{f}\left(\frac{Q_0-0.429}{\bar{E}_{\mathrm{r}}^{\alpha}}+\frac{0.429}{0.55^{\alpha}\,(1+2\alpha)}\right)}{G_{\mathrm{th\,smp}}+\frac{G_{\mathrm{e\,smp}}}{f}\left(\frac{Q_0-0.429}{\bar{E}_{\mathrm{r}}^{\alpha}}+\frac{0.429}{0.55^{\alpha}\,(1+2\alpha)}\right)} \times \right.$$

$$\left(\frac{d_{\mathrm{nom}}+\Delta d_{\mathrm{smp}}-d'_0}{d_{\mathrm{nom}}+\Delta d_{\mathrm{std}}-d'_0}\right)^2 \frac{\frac{1-e^{-\nu_{\mathrm{std}}\,h_{\mathrm{std}}\,\rho_{\mathrm{std}}}}{\nu_{\mathrm{std}}\,h_{\mathrm{std}}\,\rho_{\mathrm{std}}}}{\frac{1-e^{-\nu_{\mathrm{smp}}\,h_{\mathrm{smp}}\,\rho_{\mathrm{smp}}}}{\nu_{\mathrm{smp}}\,h_{\mathrm{smp}}\,\rho_{\mathrm{smp}}}} \frac{\left(1+\frac{h_{\mathrm{smp}}}{d_{\mathrm{nom}}+\Delta d_{\mathrm{smp}}-d'_0}\right)}{\left(1+\frac{h_{\mathrm{std}}}{d_{\mathrm{nom}}+\Delta d_{\mathrm{std}}-d'_0}\right)}\, m_{\mathrm{std}}(1-\eta_{\mathrm{std}})\, w_{\mathrm{std}} +$$

$$\left. -m_{\mathrm{blank}}\, w_{\mathrm{blank}} \right) \frac{1}{m_{\mathrm{smp}}\left(1-\eta_{\mathrm{smp}}\right)}, \qquad (1)$$

where, w is the mass fraction, n_{p} is the peak net area of the selected gamma emission, t_{c} is the real counting time, t_{l} is the live counting time, μ is the excess counting loss constant, $\lambda = \ln(2)/t_{1/2}$, is the decay constant, $\Delta t_{\mathrm{d}} = t_{\mathrm{d\,smp}} - t_{\mathrm{d\,std}}$ is the decay time difference between sample and standard, β is the vertical count rate gradient per unit of distance due to neutron flux gradient, Δl is the distance between sample and standard center of masses during irradiation, G_{th} is the thermal self-shielding, G_{e} is the epithermal self-shielding, f is the thermal to epithermal flux ratio, Q_0 is the resonance integral to 2200 m s^{-1} cross-section ratio, E_{r} is the effective resonance energy, α is the correction to the E^{-1} epithermal flux trend, d_{nom} is the nominal counting position, d'_0 is the point-of-action within the detector, Δd is the difference between experimental and nominal counting distance, v is the mass attenuation coefficient, h is the height, ρ is the density, m is the mass and η is the moisture mass fraction; subscripts std and smp refer to standard and sample.

Q_0 and $\bar{E}_r$ values reported in the k0 database [2] and f and α values previously measured at the irradiation channels of the TRIGA Mark II reactor of the University of Pavia [3] are used.

Other than uncertainty budget outputs, the software also issued analysis savefiles for data quality aim; they allow to recall and replicate the whole Rel-INRIM analysis at any moment, if required.

3.1 Neutron flux gradient correction

The β value was evaluated by the Rel-INRIM software through calculation of the specific count rates between each couple of As standards adjacent to the sample. The neutron flux gradient correction, $\frac{1}{1+\beta\,\Delta l'}$, is automatically applied. Steeper neutron flux gradients were observed going towards the top of irradiation containers placed in channels LS-25 and LS-26 while LS-27 showed a more erratic behavior along the whole axis. Accordingly, the largest flux gradient corrections, calculated in those areas, were in the order of |1| %, with negligible uncertainties, evaluated considering a 4.1 mm distance between the center of mass of a sample and its corresponding standard, Δl.

3.2 Self-shielding and absorption corrections

Sample, $G_{\mathrm{th\ smp}}$ and $G_{\mathrm{e\ smp}}$, and standard, $G_{\mathrm{th\ std}}$ and $G_{\mathrm{e\ std}}$, self-shielding correction factors were set to 1 because the automatic calculation is not yet implemented in the Rel-INRIM software. However, we do not expect significant departures from the unity value because the matrix is an organic material.

The sample self-absorption $\frac{1-e^{-\nu_{\mathrm{smp}}\,h_{\mathrm{smp}}\,\rho_{\mathrm{smp}}}}{\nu_{\mathrm{smp}}\,h_{\mathrm{smp}}\,\rho_{\mathrm{smp}}}$ correction factor was set to 1 with negligible uncertainty based on results obtained with similar samples (oyster tissue CRM). For that reason, despite density and height were included in the analysis, they had no effect in the evaluation of results. The standard self-absorption $\frac{1-e^{-\nu_{\mathrm{std}}\,h_{\mathrm{std}}\,\rho_{\mathrm{std}}}}{\nu_{\mathrm{std}}\,h_{\mathrm{std}}\,\rho_{\mathrm{std}}}$ was evaluated by the software resulting in the unity value with negligible uncertainty.

3.3 Counting position and geometry corrections

Counting position $\left(\frac{d_{\mathrm{nom}}+\Delta d_{\mathrm{smp}}-d'_0}{d_{\mathrm{nom}}+\Delta d_{\mathrm{std}}-d'_0}\right)^2$ and geometry $\frac{\left(1+\frac{h_{\mathrm{smp}}}{d_{\mathrm{nom}}+\Delta d_{\mathrm{smp}}-d'_0}\right)}{\left(1+\frac{h_{\mathrm{std}}}{d_{\mathrm{nom}}+\Delta d_{\mathrm{std}}-d'_0}\right)}$ corrections were calculated by the Rel-INRIM software based on information derived from detector efficiency characterization, d_{nom} and d'_0, and knowledge of experimental counting positions, Δd_{smp} and Δd_{std}, and samples' height, h_{smp} and h_{std}.

The 0.4 mm value was assigned to both the Δd_{smp} and Δd_{std} and obtained as the difference between 4.00 mm (Figure 8) and 3.6 mm (distance between the nominal counting position and the top of the counting spacer).

3.4 Excess counting loss correction

Sample $e^{\mu\left(1-t_{\mathrm{l\ smp}}/t_{\mathrm{c\ smp}}\right)}$ and standard $e^{\mu\left(1-t_{\mathrm{l\ std}}/t_{\mathrm{c\ std}}\right)}$ excess counting loss correction factors were calculated and applied by the Rel-INRIM software based on the 0.025 value of μ previously evaluated for the ORTEC detector through acquisition of a ^{137}Cs γ-source in multiple dead time conditions. Despite the

noticeable differences in dead time between sample and standard spectra, the corrections turned out to be negligible.

3.5 Interferences and blank corrections

A long background spectrum was acquired which confirmed the complete absence of background gamma peaks interfering with the 559.1 keV ^{75}As peak. Inspection of samples' spectra acquired during the analysis did not reveal the presence of radionuclides emitting interfering gamma. Accordingly, no correction was applied due to interferences.

In addition, a spectrum was acquired for one of the dummies in the irradiation stack confirming the absence of quantifiable signal due to presence of As, thus correction for As in the blank wasn't applied either.

4. Results

Uncertainty budgets of the As mass fraction measured twice in the 9 samples and carried out at d_{80} and d_{40} counting positions were obtained. The results are reported in Table 3 and plotted in Figure 11.

Table 3: As mass fraction from measurements performed at d_{80} and d_{40} counting positions, w_{As}, and averages of mass fraction measurements referred to the same sample, $\hat{w}_{As}$. Absolute and relative uncertainties are reported as combined standard uncertainties.

code	position	w_{As} / g g^{-1}	$u_r(w_{As})$ / 1	$\hat{w}_{As}$ / g g^{-1}	$u_r(\hat{w}_{As})$ / 1
A_2	d_{80}	1.316(29) × 10^{-6}	2.2 %	1.313(20) × 10^{-6}	1.5 %
	d_{40}	1.309(28) × 10^{-6}	2.1 %		
A_4	d_{80}	1.324(30) × 10^{-6}	2.3 %	1.331(19) × 10^{-6}	1.5 %
	d_{40}	1.336(25) × 10^{-6}	1.9 %		
A_6	d_{80}	1.317(30) × 10^{-6}	2.3 %	1.339(19) × 10^{-6}	1.5 %
	d_{40}	1.356(26) × 10^{-6}	1.9 %		
B_2	d_{80}	1.327(29) × 10^{-6}	2.2 %	1.353(19) × 10^{-6}	1.4 %
	d_{40}	1.374(26) × 10^{-6}	1.9 %		
B_4	d_{80}	1.307(28) × 10^{-6}	2.2 %	1.335(19) × 10^{-6}	1.4 %
	d_{40}	1.360(27) × 10^{-6}	2.0 %		
B_6	d_{80}	1.355(29) × 10^{-6}	2.1 %	1.322(19) × 10^{-6}	1.4 %
	d_{40}	1.297(26) × 10^{-6}	2.0 %		
C_2	d_{80}	1.318(28) × 10^{-6}	2.1 %	1.331(19) × 10^{-6}	1.4 %
	d_{40}	1.343(26) × 10^{-6}	1.9 %		
C_4	d_{80}	1.305(30) × 10^{-6}	2.3 %	1.316(20) × 10^{-6}	1.5 %
	d_{40}	1.325(27) × 10^{-6}	2.1 %		
C_6	d_{80}	1.333(29) × 10^{-6}	2.2 %	1.362(19) × 10^{-6}	1.4 %
	d_{40}	1.385(26) × 10^{-6}	1.9 %		

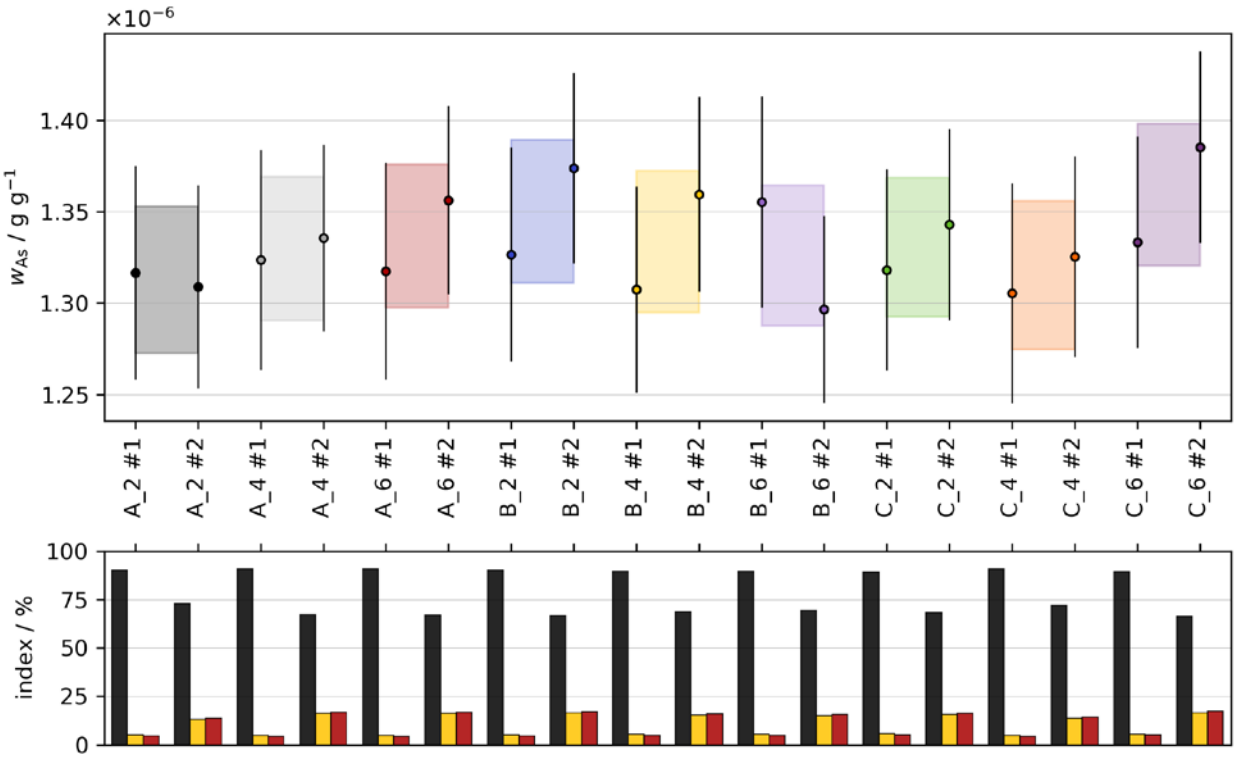

Figure 11: The upper graph reports the As mass fraction, w_{As}, measured twice in 9 samples of the comparison material both at d_{80} (suffix #1) and d_{40} (suffix #2) counting positions. Error bars and colored bands indicate expanded uncertainty (k = 2) of the data and (d_{80}, d_{40}) averages, respectively. The lower histogram reports the % contribution (index) to the combined uncertainty of the corresponding measurement due to counting statistics (black), sample position (yellow) and all other parameters (red).

Uncertainty budgets of single results highlighted a similar combined uncertainty with counting statistics as the main contributor, followed by counting position and all the remaining parameters (Figure 11, lower histogram). Since As mass fraction values obtained with the same sample at d_{80} and d_{40} are in agreement in all cases (Figure 11, upper graph), their average value and uncertainty is assigned to the corresponding sample.

As mass fraction values, y_j, quantified in the 9 samples and the corresponding average, y, are plotted in Figure 12. The scattering did not highlight any non-homogeneity of As mass fraction between samples taken from the bottle provided for the comparison.

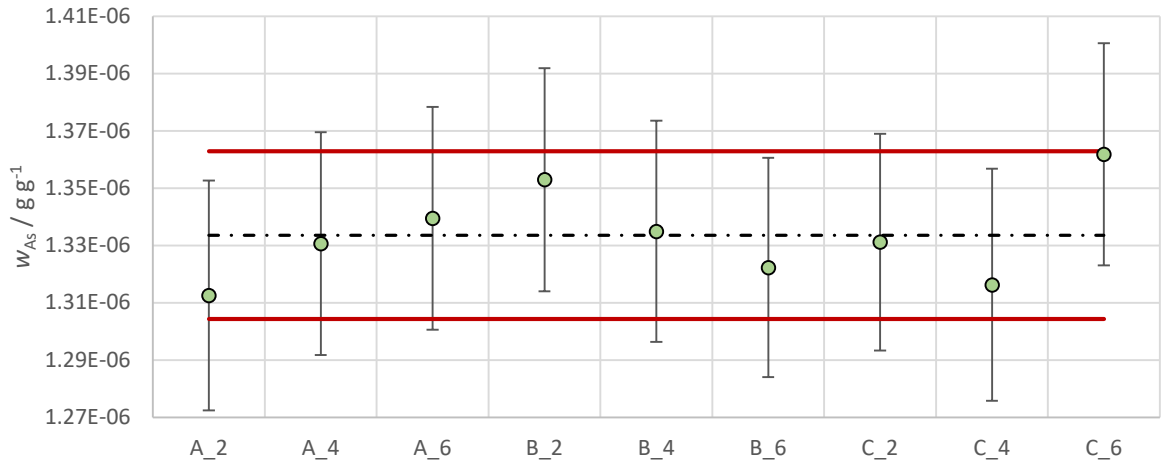

Figure 12: As mass fraction values (colored dots) quantified in 9 samples of the comparison material and their average value (black horizontal dashed line). Error bars and horizontal solid red lines indicate expanded uncertainty (k = 2) of single values and average value, respectively.

The combined uncertainty of the average, $u(y)$, is evaluated starting from uncertainty budgets of single results. In details, the variance contribution of an input quantity i, $u_i^2(y)$, eq. (11b) GUM [4], is calculated as the average of the variances of the same input quantity in single budgets, $u_i^2(y_j)$. Only in case of counting statistics the average variance is divided by number of single results, i.e. 18 in this case.

The uncertainty budget of the average is shown in Table 4. Input quantities, units, range of values, variance contribution, degree of freedom and % contribution to the combined variance (Index) are reported. The coverage factor required to express an expanded uncertainty was calculated through the evaluation of effective degrees of freedom based on the Welch-Satterthwaite formula.

Table 4: Uncertainty budget of the average As mass fraction, y. Input quantities, units, range of values, variance contribution, degree of freedom and index are reported. The expanded uncertainty at 95 % confidence level is calculated with the Welch-Satterthwaite formula.

Quantity	**Unit**	**Range of values**		**Variance**	**DoF**	**Index**
X_i	$[X_i]$	$\min(x_i)$	$\max(x_i)$	$u_i^2(y)$	ν_i	I / %
t_i	s	2.16×10^4	2.16×10^4	2.2×10^{-44}	30	0.0
$n_{p\,a}$	1	9.01×10^3	1.21×10^4	6.7×10^{-17}	30	30.9
Δt_d	s	-2.60×10^5	8.92×10^4	3.8×10^{-24}	30	0.0
$t_{c\,a}$	s	3.60×10^3	4.20×10^3	5.3×10^{-24}	30	0.0
$t_{l\,a}$	s	2.78×10^3	3.35×10^3	8.3×10^{-21}	30	0.0
m_{sm}	g	5.20×10^{-1}	5.57×10^{-1}	6.0×10^{-22}	30	0.0
η_{sm}	1	5.25×10^{-2}	5.25×10^{-2}	7.9×10^{-18}	15	3.6
$G_{th\,a}$	1	1.0	1.0	0.0	15	0.0
$G_{e\,a}$	1	1.0	1.0	0.0	15	0.0
$n_{p\,m}$	1	9.12×10^4	4.96×10^5	1.4×10^{-18}	30	0.6
$t_{d\,m}$	s	1.54×10^5	6.05×10^5	0.0	30	0.0

$t_{c\,m}$	s	1.80×10^{3}	3.60×10^{3}	1.4×10^{-23}	30	0.0
$t_{l\,m}$	s	1.67×10^{3}	3.57×10^{3}	1.6×10^{-20}	30	0.0
m_{std}	g	3.03×10^{-2}	3.12×10^{-2}	7.5×10^{-19}	30	0.3
η_{std}	1	0.0	0.0	0.0	30	0.0
w_m	g g^{-1}	9.87×10^{-4}	9.87×10^{-4}	1.6×10^{-17}	15	7.5
$G_{th\,m}$	1	1.0	1.0	0.0	15	0.0
$G_{e\,m}$	1	1.0	1.0	0.0	15	0.0
f	1	16.9	16.9	4.4×10^{-45}	15	0.0
α	1	1.36×10^{-3}	1.36×10^{-3}	6.2×10^{-46}	15	0.0
Δd_a	mm	4.00×10^{-1}	4.00×10^{-1}	3.5×10^{-17}	15	15.9
ν_a	mm^2 g^{-1}	1.00×10^{-4}	1.00×10^{-4}	0.0	15	0.0
h_a	mm	6.5	6.5	2.0×10^{-18}	15	0.9
ρ_a	g mm^{-3}	1.00×10^{-3}	1.10×10^{-3}	7.6×10^{-29}	15	0.0
Δd_m	mm	4.00×10^{-1}	4.00×10^{-1}	3.7×10^{-17}	15	17.2
ν_m	mm^2 g^{-1}	7.70×10^{-3}	7.70×10^{-3}	2.1×10^{-28}	15	0.0
h_m	mm	1.00×10^{-1}	1.00×10^{-1}	5.8×10^{-19}	15	0.3
ρ_m	g mm^{-3}	1.00×10^{-5}	1.10×10^{-1}	2.4×10^{-29}	15	0.0
β	mm^{-1}	-2.62×10^{-3}	2.33×10^{-3}	6.0×10^{-18}	15	2.8
Δl	mm	4.1	4.1	2.1×10^{-19}	15	0.1
μ	1	2.51×10^{-2}	2.51×10^{-2}	1.1×10^{-19}	15	0.1
$w_{a\,blank}$	g g^{-1}	0.0	0.0	0.0	15	0.0
m_{blank}	g	0.0	0.0	0.0	30	0.0
λ	s^{-1}	7.34×10^{-6}	7.34×10^{-6}	4.2×10^{-17}	30	19.4
Q_0	1	13.6	13.6	8.8×10^{-19}	15	0.4
E_r	eV	1.06×10^{2}	1.06×10^{2}	3.9×10^{-28}	15	0.0
d'_0	mm	-29.6	-29.6	1.1×10^{-19}	15	0.1

Quantity	**Unit**	**Value**	**Std unc**	**DoF**	**Exp unc (95 %)**
Y	**[*y*]**	***Y***	***u*(*y*)**	ν_i	***U*(*y*)**
w_a	g g^{-1}	**1.334×10^{-6}**	**1.5×10^{-8}**	**116**	**2.9×10^{-8}**

From the inspection of the uncertainty budget the main contributors to the combined uncertainty resulted to be (i) sample counting statistics, (ii) decay constant of ^{75}As, (iii) standard counting position, (iv) sample counting position and (v) standard mass fraction. The magnitude of the contribution is shown in Figure 8.

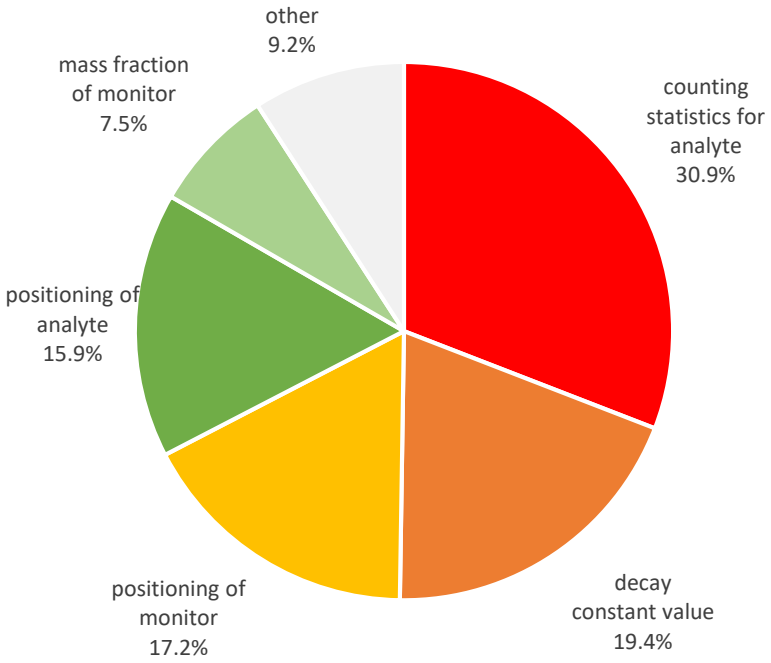

Figure 8: Pie chart showing the contribution of the most important input quantities to the combined variance based on the uncertainty budget reported in Table 4.

To conclude, the resulting interval for As mass fraction in shrimp sample can be alternatively expressed as 1.334(15) × 10^{-6} g g^{-1}, where the number in parenthesis is the numerical value of the combined standard uncertainty (u_c) referred to the corresponding last digits of the quoted result; or as the range (1.334 ± 29) × 10^{-6} g g^{-1}, where the number following the symbol ± is the numerical value of an expanded uncertainty (U = k u_c) determined from a coverage factor k = 1.98 based on the t-distribution with v = 116 effective degrees of freedom and defines an interval estimated to have a level of confidence of 95 %.

5. Conclusion

This document reports the measurement of As mass fraction in seafood sample, performed at INRIM, with relative-INAA technique. The achieved 1.1 % combined relative standard uncertainty for the As quantification at ppm level was possible due to the adopted experimental setup and the relatively high number of investigated replicates which allowed to reduce the counting statistics component of the combined uncertainty.

The results obtained in this analysis will provide data within the CCQM APMP.QM-S19 comparison focused on toxic metals in seafood samples and support the corresponding INRIM Calibration and Measurement Capability: CMC PT-QM.11.2-01.

6. References

[1] Di Luzio M, Oddone M, D'Agostino G; "Developments of the k0-INRIM measurement model" [submitted to Measurement Science and Technology]

[2] k_0-database http://www.kayzero.com/k0naa/k0naaorg/Nuclear_Data_SC/Nuclear_Data_SC.html

[3] Di Luzio M, D'Agostino G, Oddone M, Salvini A; Vertical variations of flux parameters in irradiation channels at the TRIGA Mark II reactor of Pavia Progress in Nuclear Energy 113 (2019) 247–254

[4] Evaluation of measurement data — Guide to the expression of uncertainty in measurement, JCGM 100:2008